Predicting the high-pressure phase equilibria of binary mixtures of n-alkanes using the SAFT-VR approach

Clare M^c^Cabe, Amparo Galindo, Alejandro Gil-Villegas, and George Jackson

Department of Chemistry,
University of Sheffield,
Sheffield, S3 7HF, UK.

Running title: Theory of phase equilibria of n-alkanes
Number of pages: 12 (including figure captions)
Figures: 4
Tables: 1

PACS numbers: 05.70.Fh, 64.10.+h, 64.70.-p.

Abstract

The phase behaviour of selected alkane binary mixtures are studied using SAFT-VR, a version of the statistical associating fluid theory (SAFT). We treat the molecules as chains formed from united-atom hard-sphere segments, with a square-well potential of variable range to describe the attractive interactions. We use a simple relationship between the number of carbon atoms in the n-alkane molecule and the number of segments in the united atom chains in order to predict the phase behaviour of n-butane with other n-alkanes. The calculated vapour pressures and saturated liquid densities of the pure components are fitted to experimental data from the triple point to the critical point and the parameters are scaled to the critical points. We use the Lorentz-Berthelot mixing rule for the unlike interactions. We predict the phase behaviour of n-butane + n-alkane binary mixtures, concentrating mainly on the critical region. The gas-liquid critical lines predicted by SAFT-VR for the n-alkane mixtures are in excellent agreement with the experimental data, and improve significantly on the results obtained with the simpler SAFT-HS approach where the attractive interactions are treated at the mean-field level.

1. Introduction

The high-pressure phase behaviour of mixtures are important in the design and development of extraction and separation processes, such as supercritical fluid extraction, coal conversion, and chromatography (see the reviews of McGlashan [1], Franck [2], Pitzer [3], and Schneider [4]). The properties of mixtures containing n-alkanes are obviously of interest to the petroleum industry, the seperation of petroleum and natural gas for instance, but also provides an opportunity to examine the effect of chain length on phase behaviour.

The similar chemical nature of the n-alkane molecules is reflected in their phase behaviour. If one uses the classification of Scott and van Konynenburg [5], the systems are classified as displaying type I phase behaviour. Type I systems exhibit a continuous gas-liquid critical line connecting the critical points of the two pure components, and no liquid-liquid immiscibility is observed. As expected for binary mixtures of a homologous series, a deviation from type I phase behaviour is only observed when the ratio of the critical points of the two components exceeds a certain value. For binary mixtures of methane partial immiscibility of the two components is observed with n-hexane [6]. For ethane this change in phase behaviour occurs at higher carbon numbers [7].

Accurate mixture data for the whole pTx surface is invaluable in the testing of any theoretical model designed to predict phase behaviour. Extensive experimental work on phase equilibria of the n-alkanes has been published, mainly in the 1960s and 70s [8], but some dating back as far as the early 30s. Early work was carried out at low pressures, but as the interest in high pressure phase equilibria grew, and technology advanced, we now have extensive experimental data over wide temperature and pressure ranges.

In this paper we use a version of the statistical associating fluid theory (SAFT) [9] to predict the high-pressure phase equilibria of binary mixtures of alkanes. The SAFT approach has been used extensively to examine fluid phase equilibria (see reference [10] for a recent overview). In the original SAFT expressions the molecules are treated as chains formed from Lennard-Jones segments. The approach was extended recently to potentials with a variable attractive range (SAFT-VR) [11]. A simpler version of the theory (SAFT-HS) where the molecules are chains of hard-sphere segments and the attractive interactions are treated at the mean-field level of van der Waals has also been used with some success for aqueous solutions of n-alkanes [10] and for mixtures containing hydrogen fluoride [12]. Here, we examine the adequacy of the SAFT-HS and SAFT-VR approaches in describing the fluid phase equilibria of mixtures of n-alkanes.

2. Models and Theory

The n-alkane molecules are represented by a simple united atom model: m hard-spherical segments of diameter σ tangentially bonded together to form chains. The attractive interactions are included with a square-well potential of variable width λ and depth ϵ. A simple empirical relationship, proposed in earlier work [13, 14, 10] is used to determine the number of such segments in relation to the number of carbon atoms in the molecule: $m = \frac{1}{3}(C-1)+1$. This relationship gives a reasonable description of the critical temperatures and pressures of the homologous series of n-alkanes, however it is too simplistic to reproduce the finer details, such as the anomalously low critical pressure of methane [14].

In this work the phase equilibria of binary n-alkane mixtures was studied using the SAFT-VR theory with a square-well potential [11]. We will only summarise the main expressions of the SAFT-VR theory for the square-well potential; and the reader should consult reference [11] for details. The general equation for mixtures of chain molecules formed from hard-core segments with attractive interactions is given; the contribution due to association is not included for the n-alkane systems. The Helmholtz free energy A for an n-component mixture of chain molecules can be separated into the various contributions as

$$\frac{A}{NkT} = \frac{A^{IDEAL}}{NkT} + \frac{A^{MONO.}}{NkT} + \frac{A^{CHAIN}}{NkT}, \tag{1}$$

where N is the total number of molecules, T is the temperature, and k is the Boltzmann constant. There is no need to include the association term since we are dealing with non-associating alkane systems. The ideal contribution to the free energy is given by a sum over all species i in the mixture [15],

$$\frac{A^{IDEAL}}{NkT} = \left(\sum_{i=1}^{n} x_i \ln \rho_i \Lambda_i^3\right) - 1, \tag{2}$$

where $x_i = N_i/N$ is the mole fraction, $\rho_i = N_i/V$ the molecular number density, N_i the number of molecules, and Λ_i the thermal de Broglie wavelength of species i, and V is the volume of the system. We can express the monomer Helmholtz free energy as

$$\begin{aligned} \frac{A^{MONO.}}{NkT} &= (\sum_{i=1} x_i m_i)\frac{A^M}{N_s kT} \\ &= (\sum_{i=1} x_i m_i) a^M, \end{aligned} \tag{3}$$

where m_i is the number of spherical segments of chain i. Using the Barker and Henderson [16] perturbation theory for mixtures with a hard-sphere reference system the monomer free energy per segment of the mixture is obtained from the expansion,

$$a^M = a^{HS} + \beta a_1 + \beta a_2, \tag{4}$$

where $\beta = 1/kT$ and each term is now for a mixture of spherical segments. The expression of Boublík [17] and Mansoori *et al.* [18] for a multicomponent mixture of hard spheres is used for the reference hard-sphere term,

$$a^{HS} = \frac{6}{\pi\rho_s}\left[\left(\frac{\zeta_2^3}{\zeta_3^2} - \zeta_0\right)\ln(1-\zeta_3) + \frac{3\zeta_1\zeta_2}{(1-\zeta_3)} + \frac{\zeta_2^3}{\zeta_3(1-\zeta_3)^2}\right], \tag{5}$$

where ρ_s is the total number density of spherical segments and ζ_l are the reduced densities defined by

$$\zeta_l = \frac{\pi\rho_s}{6}\sum_{i=1}^{n} x_{s,i}\sigma_{ii}^l. \tag{6}$$

Here, σ_{ii} is the diameter of the spherical segments of chain i, and $x_{s,i}$ is the mole fraction of segments of type i in the mixture.

The mean-attractive energy represented by the a_1 term is obtained from the sum of the partial terms corresponding to each type of pair interaction [11],

$$a_1 = \sum_{i=1}^{n}\sum_{j=1}^{n} x_{s,i}x_{s,j}a_1^{ij}, \tag{7}$$

where

$$a_1^{ij} = -\rho_s\alpha_{ij}^{VDW}g_{ij}^{HS}(\sigma_{ij};\zeta_3^{eff}), \tag{8}$$

and

$$\alpha_{ij}^{VDW} = 2\pi\varepsilon_{ij}\sigma_{ij}^3(\lambda_{ij}^3 - 1)/3 \tag{9}$$

is the van der Waals attractive constant for the $i-j$ square-well interaction,

$$u_{ij}(r) = \begin{cases} +\infty & \text{if } r < \sigma_{ij}, \\ -\varepsilon_{ij} & \text{if } \sigma_{ij} \le r < \lambda_{ij}\sigma_{ij}, \\ 0 & \text{if } r \ge \lambda_{ij}\sigma_{ij}. \end{cases} \tag{10}$$

Here, r is the distance between the two particles, σ_{ij} defines the contact distance between spheres, and ε_{ij} and λ_{ij} are the depth and the range of the square-well potential.

In equation (8), $g_{ij}^{HS}(\sigma_{ij};\zeta_3^{eff})$ is the contact value of the radial pair distribution function for a mixture of hard spheres obtained from the expression of Boublík [17],

$$g_{ij}^{HS}(\sigma_{ij};\zeta_3^{eff}) = \frac{1}{1-\zeta_3^{eff}} + 3\frac{D_{ij}\zeta_3^{eff}}{(1-\zeta_3^{eff})^2} + 2\frac{\left(D_{ij}\zeta_3^{eff}\right)^2}{(1-\zeta_3^{eff})^3}, \tag{11}$$

where for convenience the equation is written in terms of the parameter D_{ij},

$$D_{ij} = \frac{\sigma_{ii}\sigma_{jj}}{\sigma_{ii}+\sigma_{jj}}\frac{\sum_{i=1}^{n} x_{s,i}\sigma_{ii}^2}{\sum_{i=1}^{n} x_{s,i}\sigma_{ii}^3}, \tag{12}$$

and an effective packing fraction ζ_3^{eff} defined by [11]

$$\zeta_3^{eff}(\zeta_3,\lambda_{ij}) = c_1(\lambda_{ij})\zeta_3 + c_2(\lambda_{ij})\zeta_3^2 + c_3(\lambda_{ij})\zeta_3^3, \tag{13}$$

$$\begin{pmatrix} c_1 \\ c_2 \\ c_3 \end{pmatrix} = \begin{pmatrix} 2.25855 & -1.50349 & 0.249434 \\ -0.669270 & 1.40049 & -0.827739 \\ 10.1576 & -15.0427 & 5.30827 \end{pmatrix} \begin{pmatrix} 1 \\ \lambda_{ij} \\ \lambda_{ij}^2 \end{pmatrix}. \tag{14}$$

The first fluctuation term a_2 is evaluated using the local compressibility approximation for mixtures,

$$a_2 = \sum_{i=1}^{n}\sum_{j=1}^{n} x_{s,i}x_{s,j}a_2^{ij}, \tag{15}$$

where a_2^{ij} is each one of the partial fluctuation terms defined by

$$a_2^{ij} = \frac{1}{2}K^{HS}\epsilon_{ij}\rho_s\frac{\partial a_1^{ij}}{\partial \rho_s}. \tag{16}$$

K^{HS} is the hard-sphere isothermal compressibility of Percus-Yevick [19],

$$K^{HS} = \frac{\zeta_0(1-\zeta_3)^4}{\zeta_0(1-\zeta_3)^2 + 6\zeta_1\zeta_2(1-\zeta_3) + 9\zeta_2^3}. \tag{17}$$

Finally, the contribution to the free energy due to chain formation is expressed in terms of the contact value of the background correlation function [11],

$$\frac{A^{CHAIN}}{NkT} = -\sum_{i=1}^{n} x_i\,(m_i-1)\ln y_{ii}^{SW}(\sigma_{ii}), \tag{18}$$

where $y_{ii}^{SW}(\sigma_{ii}) = g_{ii}^{SW}(\sigma_{ii})\exp(-\beta\epsilon_{ii})$. We obtain $y_{ii}^{SW}(\sigma_{ii})$ from the high temperature expansion of $g_{ii}^{SW}(\sigma_{ii})$,

$$g_{ii}^{SW}(\sigma_{ii}) = g_{ii}^{HS}(\sigma_{ii}) + \beta\epsilon_{ii} g_1^{SW}(\sigma_{ii}), \tag{19}$$

where the term $g_1^{SW}(\sigma_{ii})$ is obtained from a self-consistent method for the pressure p from the Clausius theorem and from the density derivative of the Helmholtz free energy [11]:

$$\begin{aligned} g_{ii}^{SW}(\sigma_{ii}) &= g_{ii}^{HS}(\sigma_{ii}) \\ &+ \beta\varepsilon_{ii}\left[g_{ii}^{HS}(\zeta_3^{eff}) + (\lambda_{ii}^3 - 1)\frac{\partial g_{ii}^{HS}(\zeta_3^{eff})}{\partial \zeta_3^{eff}}\left(\frac{\lambda_{ii}}{3}\frac{\partial \zeta_3^{eff}}{\partial \lambda_{ii}} - \zeta_3\frac{\partial \zeta_3^{eff}}{\partial \zeta_3}\right)\right]. \end{aligned} \tag{20}$$

We should note at this point that in the SAFT-HS approach [10] one describes the attractive forces at the van der Waals level, and the hard-sphere contact value is used in the expression for the chain contribution.

Using standard thermodynamic relationships, the other thermodynamic properties such as the pressure and chemical potential can be obtained from the Helmholtz free energy. Phase equilibria requires that the temperature, pressure, and chemical potential of each component in each phase are equal; the conditions are solved with a simplex method [20].

3. Results and Discussion

The phase equilibria of the binary mixtures of n-butane with the other members of the homologous series up to n-octane have been studied in this work using SAFT-VR with a square-well potential of variable range. Theoretical phase diagrams are obtained for each system and compared directly with experimental data. In reference [11] the parameters for each pure n-alkane were obtained by fitting to the experimental data for the vapour pressure and saturated liquid density from the critical to the triple point [21]. In order to smooth these values of the range parameter λ for methane to n-octane we obtained in terms of a linear relation with the carbon number C, $\lambda = 0.02119C + 1.410$; for the longer chains this simple relationship does not hold. Furthermore, since our main interest was in the gas-liquid critical lines of these mixtures, the pure component σ and ϵ parameters were re-scaled to the experimental critical points. The final values of the parameters used in our study are given in table 1. It should be noted, however, that this re-scaling is always at the cost of poorer agreement with experimental data as we move further away from the critical region. In figure 1 we show the vapour pressures obtained with the SAFT-VR approach for methane through to n-octane, together with the corresponding experimental data [21].

The cross parameters needed for the mixture calculations are obtained from the pure component parameters: the unlike size and energy parameters are obtained using the Lorentz-Berthelot combining rule [6], and the unlike range parameter is obtained from the arithmetic mean. Figure 2 shows the pT projection for methane + n-butane which, as discussed earlier, exhibits simple type I phase behaviour: the gas-liquid critical line runs continuously from the critical point of the less volatile component, methane, to the critical point of the more volatile component, n-butane. We compare the results for the gas-liquid critical lines from the SAFT-VR (dashed line) and SAFT-HS (dotted) approaches with the experimental data [8]. With the SAFT-HS approach the predicted gas-liquid critical line reproduces the qualitative shape of the experimental data, with the maximum at the right temperature but at somewhat lower pressure. The SAFT-VR approach gives a significantly improved description of the pressure dependence. Corresponding px slices for the methane + n-butane binary mixture obtained from the SAFT-VR predictions are compared with the experimental data [22] in figure 3.

The gas-liquid critical lines obtained with the SAFT-VR approach for the seven other binary n-butane + n-alkane mixtures studied are displayed in figure 4, with the corresponding experimental data [8]. For clarity we have omitted the vapour pressure curves of each pure component. As expected, all of these systems display type I phase behaviour, with continuous critical lines from the critical point of pure n-butane to the critical point of the second component. For each system we achieve excellent agreement with the experimental data. There is a slight discrepancy in the pressure dependence, but this is only significant when the difference in chain length is at its greatest.

4. Conclusion

We have used the SAFT-VR approach to predict the high-pressure fluid phase equilibrium of binary mixtures of n-alkanes, and good agreement with experiment is obtained. Essentially this SAFT-VR approach goes beyond the van der Waals one-fluid theory. Although the simpler SAFT-HS approach provides a good description of systems with strong association (e.g., see[10] [12]), it is not suitable for an accurate representation of the phase behaviour of mixtures of n-alkanes. This is because the association interactions dominate the phase behaviour of the former systems. In the case of the n-alkanes a precise description of the dispersion forces is necessary. We will examine the change in phase behaviour observed experimentally from type I to type IV for the mixture of methane + n-hexane with the SAFT-VR approach in a future paper.

CM^{c}C thanks Sheffield University for the award of a UGC Scholarship, AG thanks Sheffield University and ICI Chemicals and Polymers for a Roberts-Boucher Scholarship, and AGV thanks the Engineering and Physical Sciences Research Council (EPSRC) for funding a Research Fellowship. AGV is now funded by the ICI Strategic Research Fund as a Senior Research Fellow. We also acknowledge support from the European Commission, the Royal Society, and the Computational and ROPA Initiatives of the EPSRC for the provision of computer hardware.

References

[1] McGlashan, M. L., *Pure Appl. Chem.*, **1985**, *57*, 89; *J. Chem. Thermo.*, **1985**, *17*, 301.

[2] Frank, E. U., *Pure Appl. Chem.*, **1987**, *59*, 25; *J. Chem. Thermo.*, **1987**, *19*, 225.

[3] Pitzer, K. S., *Pure Appl. Chem.*, **1989**, *61*, 979; *J. Chem. Thermo.*, **1989**, *21*, 1.

[4] Schneider, G. M., *Pure Appl. Chem.*, **1991**, *63*, 1313.

[5] Scott, R. L., and van Konynenburg, P. H., *Discuss. Faraday Soc.*, **1970**, *49*, 87; van Konynenburg, P. H., and Scott, R. L., *Philos. Trans. R. Soc. A*, **1980**, *298*, 495.

[6] Rowlinson, J. S., and Swinton, F. L., *Liquids and Liquid Mixtures*, 3rd Edition, (Butterworth Scientific, London 1982).

[7] Peters, C. J., Lichtenthaler, R. N., and de Swaan Arons, J., *Fluid Phase Equilibria*, **1986**, *29*, 495.

[8] Hicks, C. P., and Young, C. L., *Chem. Revs.* **1975**, *75*, 119.

[9] Chapman, W. G., Gubbins, K. E., Jackson, G., and Radosz, M., *Ind. Eng. Chem. Res.*, **1990**, *29*, 1709; Chapman, W. G., Gubbins, K. E., Jackson, G., and Radosz, M., *Fluid Phase Equilibria*, **1989**, *52*, 31.

[10] Galindo, A., Whitehead, P. J., Jackson, G., and Burgess, A. N., *J. Phys. Chem.* , **1996**, *100*, 6781.

[11] Gil-Villegas, A., Galindo, A., Whitehead, P. J., Mills, S. J., Jackson, G., and Burgess, A. N., *J. Chem. Phys.*, **1996**, *106*, 4168.

[12] Galindo, A., Whitehead, P. J., Jackson, G., and Burgess, A. N., *J. Phys. Chem. B*, **1997**, *101*, 2082.

[13] Jackson, G., Gubbins, K. E., *Pure Appl. Chem.* **1989**, 61, 1021.

[14] Archer, A. L., Amos, M. D., Jackson, G., McLure, I. A., *Int. J. Thermophys.*, **1996**, *17*, 201.

[15] Hansen, J. P., and McDonald, I. R., *Theory of Simple Liquids*, 2nd ed., (Academic Press, 1986).

[16] Leonard, P. J., Henderson, D., Barker, J. A., *Trans. Faraday Soc.* **1970**, *66*, 2439.

[17] Boublík, T., *J. Chem. Phys.*, **1970**, *53*, 471.

[18] Mansoori, G. A., Carnahan, N. F., Starling, K. E., and Leland, T. W., *J. Chem. Phys.*, **1971**, *54*, 1523.

[19] Reed, T. M., and Gubbins, K. E., *Applied Statistical Mechanics*, McGraw-Hill (1973).

[20] Press, W. H., Teukolsky, S. A., Vetterling, W. T., and Flannery, B. P., *Numerical Recipes in Fortran*, 1st ed., (Cambridge University Press, 1986).

[21] Smith, B. D., and Srivastava, R., *Thermodynamic Data for Pure Compounds*, (Elsevier, London 1986).

[22] Kahre, L. C., *J. Chem. Eng. Data*, **1974**, *19*, 67.

Table 1. Optimised square-well intermolecular potential parameters for n-alkanes. m is the number of spherical segments in the model, λ the range parameter, σ the diameter of each segment, and ϵ the well depth. $T_c^* = kT_c b/\alpha$ and $P_c^* = P_c b^2/\alpha$ are the reduced critical temperature and pressure, where $\alpha = 4b\epsilon(\lambda^3 - 1)$ and $b = \pi\sigma^3/6$.

Substance	m	λ	σ (Å)	ϵ/k (K)	T_c^*	P_c^*
CH_4	1	1.431	4.100	161.2	0.153137	0.00964883
C_2H_6	1.33	1.452	4.227	223.4	0.165831	0.00758847
C_3H_8	1.67	1.473	4.331	238.9	0.176321	0.00625476
C_4H_{10}	2.0	1.494	4.403	246.7	0.184545	0.00533612
C_5H_{12}	2.33	1.515	4.464	247.7	0.191445	0.00464107
C_6H_{14}	2.67	1.536	4.497	244.8	0.197589	0.00407946
C_7H_{16}	3.0	1.557	4.535	240.1	0.202693	0.00363171
C_8H_{18}	3.33	1.578	4.560	234.3	0.207210	0.00325824

Figure 1. Vapour pressures for methane through to n-octane. The circles represent the experimental data [21]. The continuous curves represent the SAFT-VR results obtained using parameters fitted to both vapour pressure and saturated liquid density data and re-scaled to the critical temperature and pressure of each pure component.

Figure 2. The pT projection for the binary mixture of methane (1) + n-butane (2) compared with the SAFT predictions. The circles represent the experimental values for the vapour pressures of methane and butane [21], and the triangles the gas-liquid critical points [8]. The continuous curves represent the SAFT-VR vapour pressures for the pure components, the dashed curve corresponds to SAFT-VR gas-liquid critical line, and the dotted curve that predicted by SAFT-HS.

Figure 3. px slices at temperatures of 21.11° C (294.26 K), 54.44° C (327.59 K), 87.78° C (360.93 K), 121.11° C (394.26 K) and 104.44° C (377.59 K) (from the outer to the inner curves) for the methane (1) + n-butane (2) binary mixture compared with the SAFT-VR predictions. The continuous curves represent the calculated coexistence curves and the diamonds the experimental data [22].

Figure 4. The gas-liquid critical lines for the binary mixtures of n-butane + n-alkanes. The triangles represent the experimental data, and the dashed lines the theoretical prediction using the SAFT-VR approach.

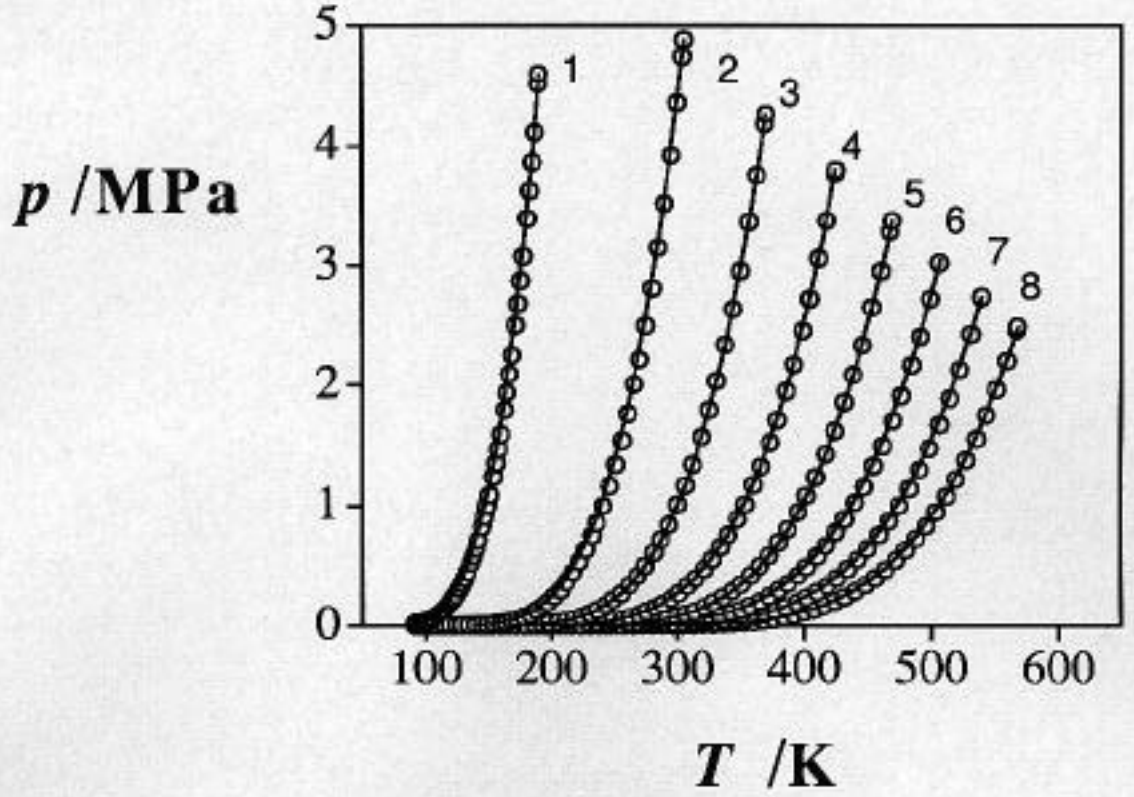

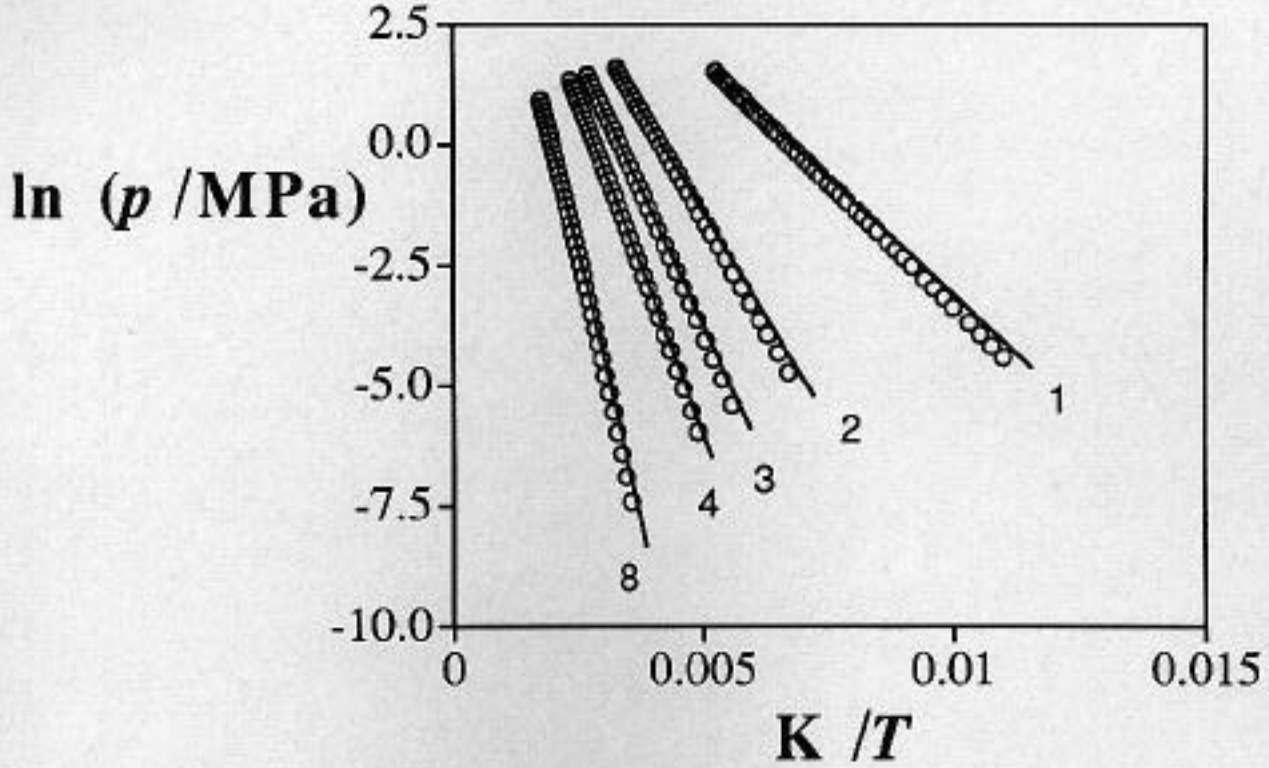

McCabe et al Fig 1

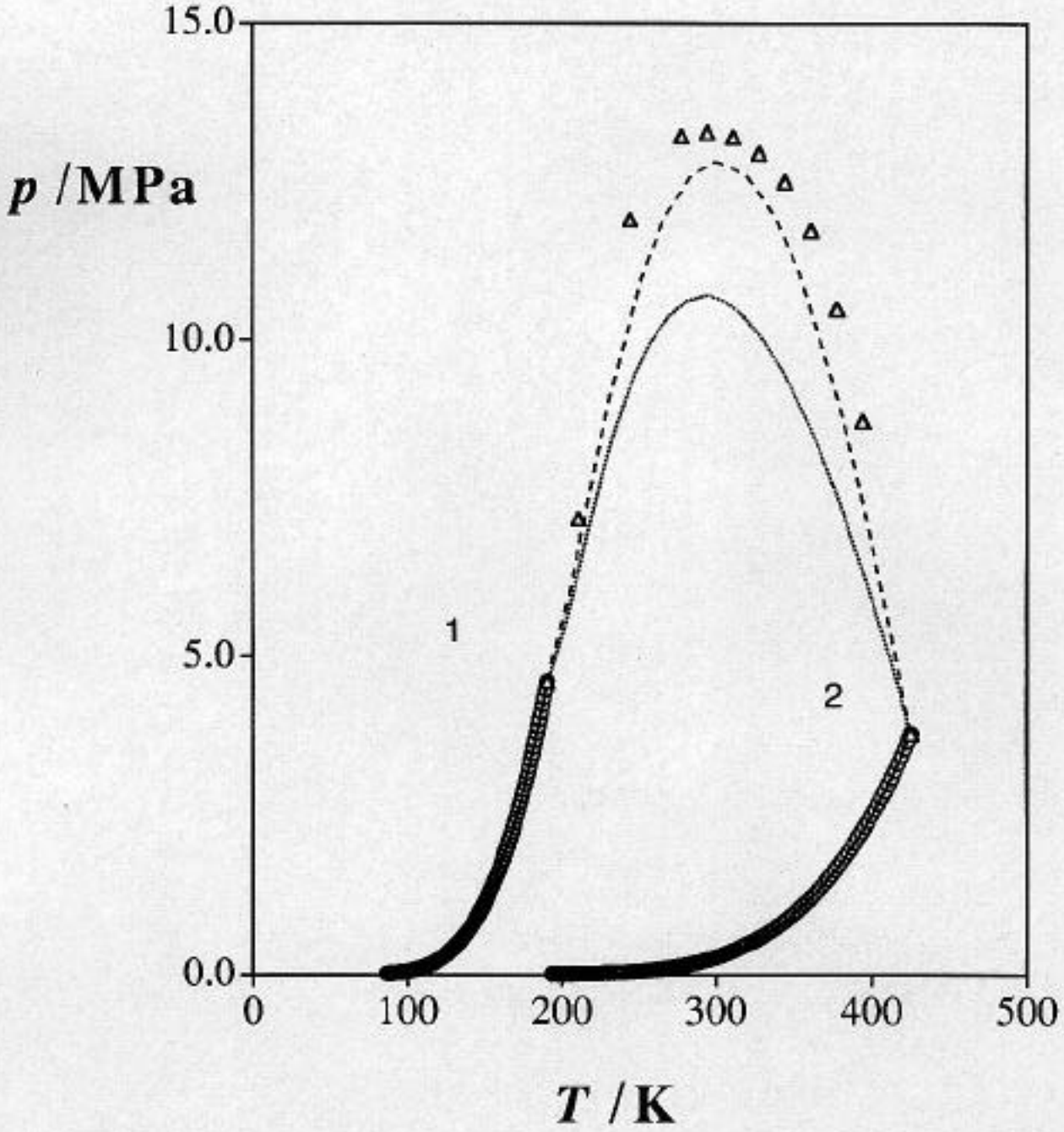

McCABE et al FIG 2

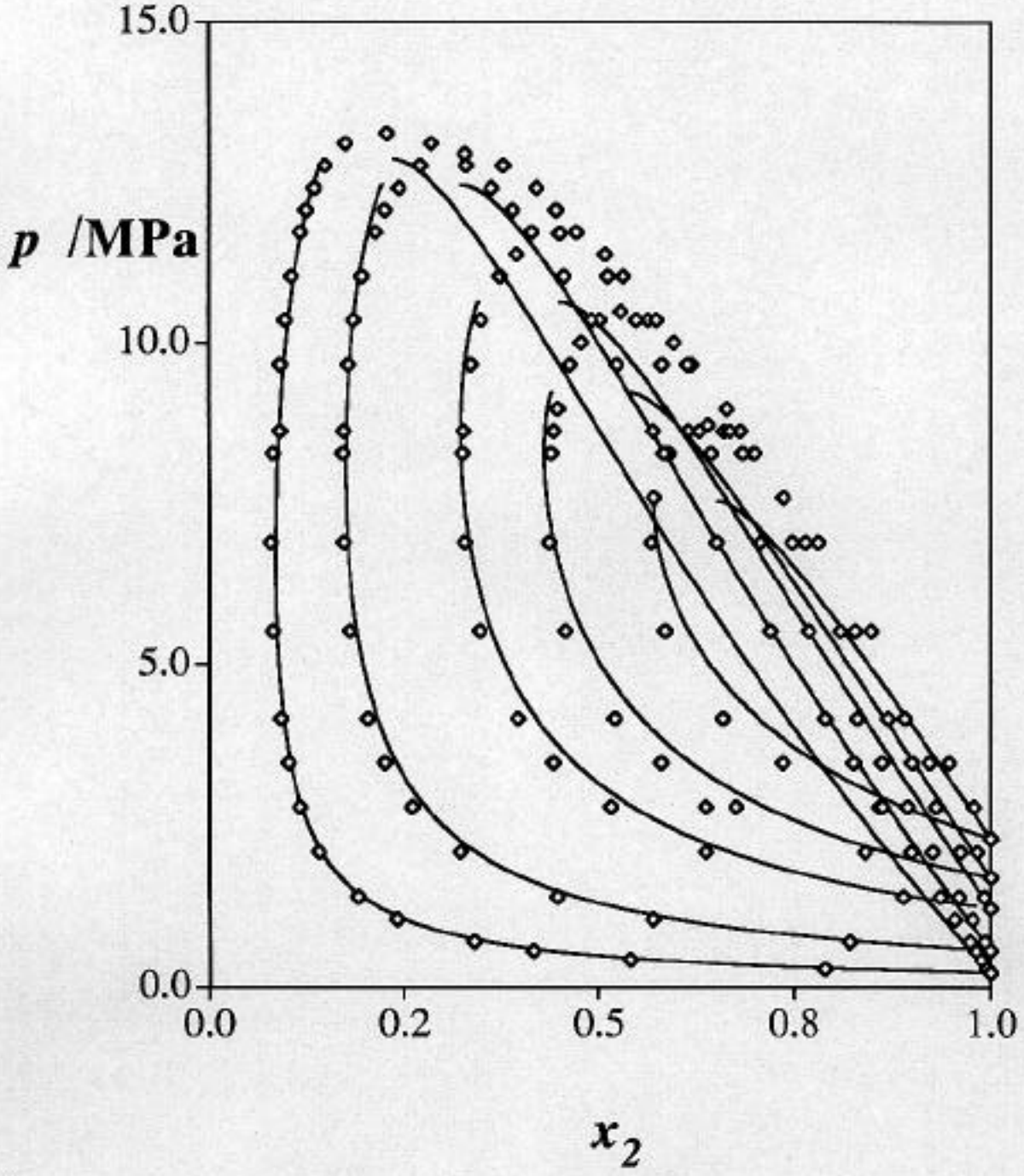

McCABE et al Fig 3

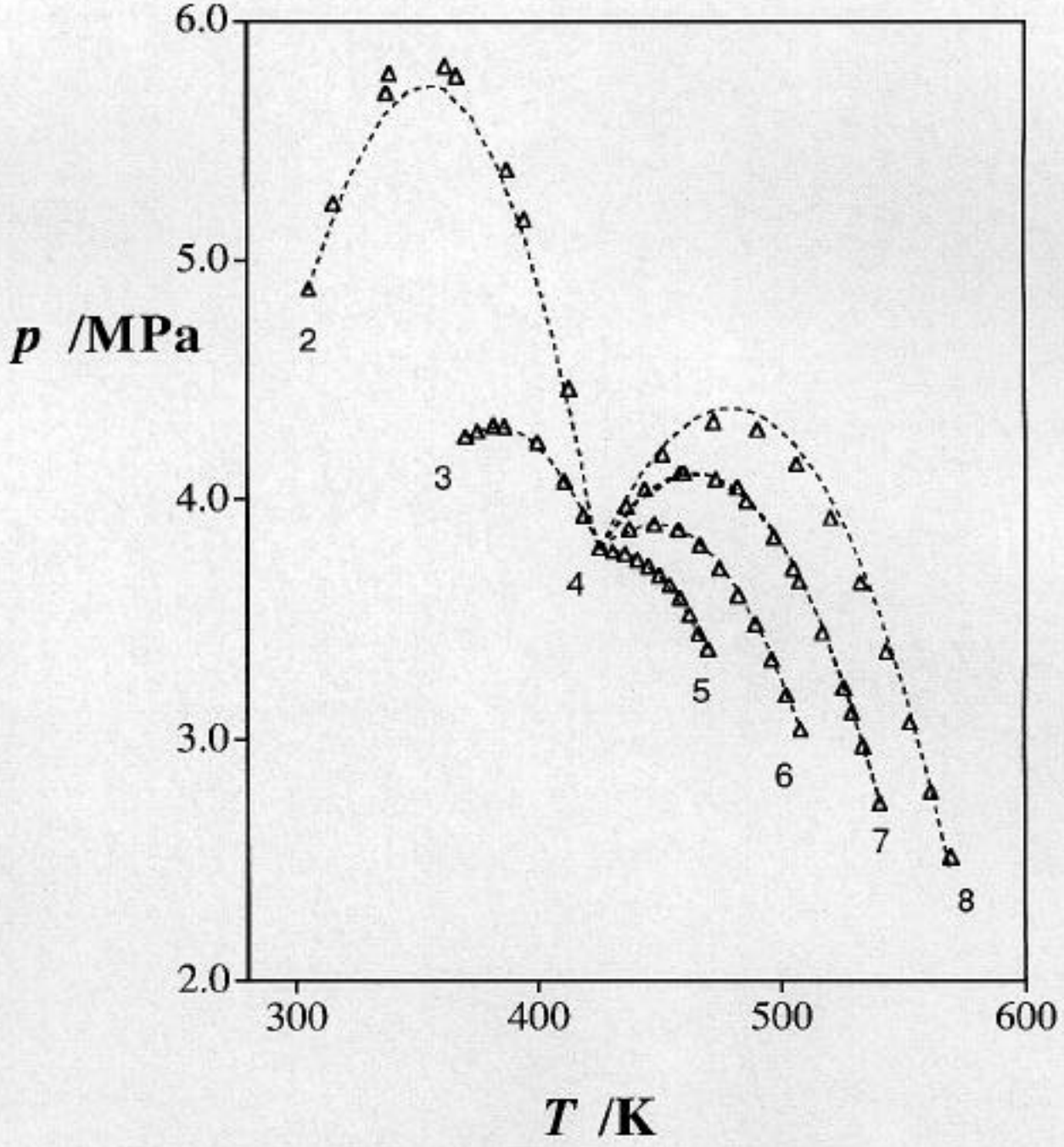

McCabe et al Fig 4